

Activity of silica-alumina for the conversion of polyethylene into tunable aromatics below pyrolytic temperatures

Makenna L. Pennel,¹ Anjani K. Maurya,² Amani M. Ebrahim,² Christopher J. Tassone,² Matteo Cargnello^{*3}

¹ Department of Chemistry, Stanford University, Stanford, CA 94305, United States

² SLAC National Accelerator Laboratory, Stanford Synchrotron Radiation Lightsource, Menlo Park, CA 94025, United States

³ Department of Chemical Engineering and SUNCAT Center for Interface Science and Catalysis, Stanford University, Stanford, CA 94305, United States

Keywords: silica-alumina; plastics upcycling; sustainable recycling; alkyl aromatics; heterogeneous catalyst; metal-free catalyst

Abstract

Plastic waste is a mounting problem that lacks global strategy, largely due to inadequate recycling capabilities. One alternative gaining traction in the heterogeneous catalysis community is the upcycling of polyolefins into value-added products, such as the hydrogen-free conversion to alkylaromatic compounds over Pt/Al₂O₃. Here, we examined the activity of nominally metal-free, mesoporous silica-alumina mixed oxide materials (SiO₂-Al₂O₃) for the conversion of polyethylene into aromatic compounds at temperatures at and below 280 °C. Yields with the silica-alumina catalysts are comparable to those obtained over Pt(1 wt%)/Al₂O₃ under identical conditions, and product selectivity can be tuned by altering reaction conditions or the acid site density of the SiO₂-Al₂O₃. Notably, the fraction of polyaromatic products increases with the Brønsted acid site density of the catalyst, as does the degree of polymer deconstruction. These catalysts can be reused without regeneration and their activity improves with each recycling event, giving soluble product yields up to 83%. Preliminary work on the mechanism of the reaction suggests that acid sites are responsible for initiating depolymerization and aromatization reactions, in analogy to previous work in the literature. This work showcases the activity of SiO₂-Al₂O₃ for polyolefin deconstruction/aromatization at sub-pyrolytic temperatures and lays the foundation for future studies involving solid acid and bi-functional catalysts.

Introduction

Plastic waste is a growing global catastrophe. Over 6.9 billion metric tons have been generated since the onset of mass-produced plastic in the early 1950s— most being discarded.¹ The United States reported a dismal 8.7% recycling rate in 2018.² A similar fraction was incinerated for energy recovery (15.8%) and the rest entered either landfills or the environment, where impacts are not fully understood.³ Action is needed in many forms to curb the plastic waste problem and mitigate environmental consequences, including innovations in plastic recycling technology. Mechanical processes dominate today's recycling landscape, but polymer degradation leads to “downcycling,” limiting the prevalence of plastic recycling in its current form.

The search for a superior recycling process has spanned decades and disciplines, but to date, the most success (in terms of number of publications and patents) has come from the field of catalytic pyrolysis.⁴ This reaction is largely agnostic to the plastic feedstock, but substantial energy requirements and poor product selectivity limit its implementation outside the laboratory.^{5,6} Alternative low-temperature reactions, including monofunctional hydrogenolysis and bifunctional hydrocracking, have gained increasing attention in recent years.⁶⁻¹⁷ Unlike pyrolysis, which converts polyethylene into a mixture of products at temperatures well above 350 °C,¹⁸ hydroconversion reactions selectively produce fuel-range alkanes at significantly lower temperatures using moderate hydrogen pressures. However, questions surround the economics of these conversions, given the products are of relatively low monetary value and require 1 mole of hydrogen for every mole of C-C bonds cleaved.^{19,20}

Alternative low-temperature reactions which produce value-added products have been proposed. One prominent example is the hydrogen-free tandem hydrogenolysis/aromatization reaction pioneered by Zhang et al., which converts polyethylene into alkylaromatics using a Pt/Al₂O₃ catalyst at 280 °C. These products are valuable as lubricants and detergent precursors, and are currently produced through more energy-intensive routes.¹⁹ Adding a small amount of iron to the catalyst has been shown to further increase the yield of aromatics.²¹ A techno-economic assessment for this type of polymer conversion has not been published as of this writing, but the catalyst will undoubtedly be a cost driver given the low polymer/catalyst ratios and energy-intensive catalyst regeneration procedures detailed in the literature. Lowering catalyst costs and increasing efficiency are paramount to moving the technology forward. In a preliminary step to address these problems, we examined the activity of nominally metal-free silica-alumina mixed oxide materials (SiO₂-Al₂O₃) for the conversion of polyethylene into aromatic compounds.

Many solid acid catalysts have been tested in pyrolysis reactions for polyethylene deconstruction, including SiO₂-Al₂O₃.²²⁻²⁴ Unlike zeolites, which are microporous and have narrow pore distributions, SiO₂-Al₂O₃ is typically mesoporous— a property that is thought to improve polymer transport during reactions.^{25,26} Several studies have shown that cracking of the polyolefin chain increases with SiO₂-Al₂O₃ acidity during catalytic pyrolysis and occurs predominantly on Brønsted acid sites.^{25,24} Aromatics are known to form over acidic catalysts during short alkane cracking and have been observed in polyolefin cracking as well.^{27,28} Notably, Ohkita et al. tested a series of SiO₂-Al₂O₃ catalysts in reactions with thermally-degraded polyethylene vapor and found that the yield of aromatics increased with the number of acid sites.²⁹

To the best of our knowledge, however, the conversion of polyolefins to aromatics over SiO₂-Al₂O₃ has not been investigated in the polymer melt phase— where transport effects have been extensively documented^{25,12,30,31} — or at sub-pyrolytic temperatures.

Herein, we demonstrate that nominally metal-free SiO₂-Al₂O₃ deconstructs polyethylene into smaller, aromatic molecules under identical conditions as those used by Zhang et al. during reactions with Pt/Al₂O₃. Yields are comparable, the catalyst can be reused without regeneration, and product selectivity can be tuned by altering reaction conditions, the acid site density of the SiO₂-Al₂O₃, or the number of catalyst reuse events.

Results and Discussion

In preliminary experiments, low molecular weight polyethylene ($M_w \sim 3000$ g mol⁻¹) was loaded in stainless steel mini reactors (approximately 10 mL volume, Figure S1) in an argon atmosphere with a catalyst, either commercial Pt(1 wt %)/Al₂O₃ or SiO₂-Al₂O₃ (10 wt % silica, labeled 10SA). The reaction was run for 24 hours at 280 °C and non-gaseous products were extracted with hot chloroform. Reactions with Pt(1 wt %)/Al₂O₃ and 10SA exhibited similar mass yield profiles post-extraction, with 56 wt % and 45 wt % chloroform-soluble product yields, respectively (Figure 1a). γ -Al₂O₃ performed poorly by comparison, resulting in predominantly chloroform-insoluble residue (55 wt %) and minimal soluble products. Gaseous products that completed the mass balances were not collected in these preliminary experiments (see more below).

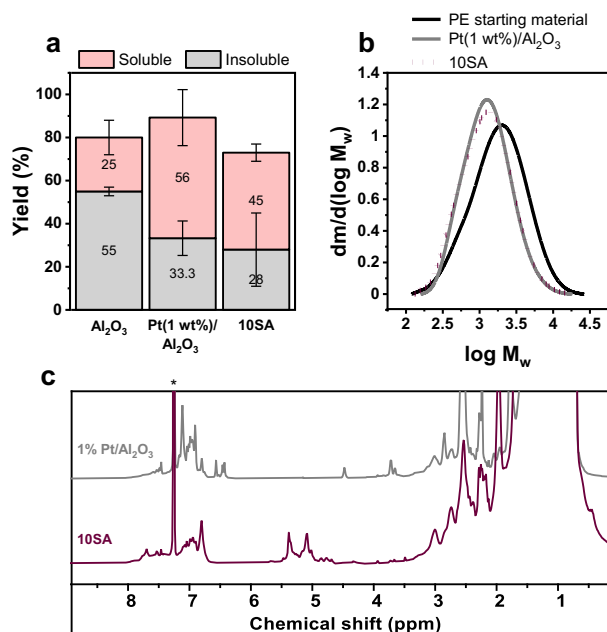


Figure 1. (a) Chloroform-soluble and -insoluble yields (wt %) after reactions with PE (280 °C, 24 h). (b) GPC profiles and (c) ¹H NMR spectra of the chloroform-soluble products. *CDCl₃ solvent signal

The chloroform-soluble products were further characterized with gel permeation chromatography (GPC, Figure 1b). The reaction with γ -Al₂O₃ resulted in a minimal reduction in average molecular weight (23%, $\langle M_w \rangle = 1964 \text{ g mol}^{-1}$) and changes during a control experiment with only polyethylene in the reactor were negligible (Figure S2). On the other hand, a notable reduction in average molecular weight during reactions with Pt/Al₂O₃ (35%, $\langle M_w \rangle = 1658 \text{ g mol}^{-1}$) and 10SA (36%, $\langle M_w \rangle = 1639 \text{ g mol}^{-1}$) was observed. The dispersity also decreased from that of the starting material ($D = 2.05$) in both cases ($D = 1.68$ for Pt/Al₂O₃ and 1.79 for 10SA).

While the GPC M_w distribution is similar in both instances, proton NMR analysis suggests product selectivity differs (Figure 1c). Prominent peaks in the 4.7-5.8 ppm region appear in the 10SA reaction product spectrum, corresponding to olefins.³² There are no features in this region in the case of Pt/Al₂O₃. There are also broad signals in the 6.5-9.0 ppm region for both the Pt/Al₂O₃ and 10SA reaction products, indicative of protons bound to aromatic rings.¹⁹ Control experiments with γ -Al₂O₃ and PE alone do not produce products with quantifiable ¹H NMR peaks in the aromatic region (Figure S3). Integration indicates aromatics are produced in similar amounts during reactions with 10SA and Pt/Al₂O₃ (aromatic/total proton ratio = 0.005 ± 0.001 and 0.0068 ± 0.0001 for 10SA and Pt/Al₂O₃, respectively), but the relative compositions differ. Pt/Al₂O₃ produces mostly monoaromatic products (corresponding to signals from 6.5-7.4 ppm), while 10SA produces products with prominent features in the polyaromatic region as well (broad signal from 7.4-9.0 ppm), indicative of fused rings.¹⁹ This difference in product compositions is supported by integration of the ¹H NMR aromatic region: the monoaromatic/polyaromatic proton ratio is 4.4 in the case of Pt/Al₂O₃, and 2.9 for 10SA. We tried to further understand the composition of the chloroform-soluble products, but the compounds could not be analyzed using traditional mass spectrometry techniques due to ionization difficulties.

The available evidence suggests 10SA deconstructs polyethylene into shorter aromatic compounds under the same reaction conditions as Pt(1 wt %)/Al₂O₃ and exhibits similar performance without added noble metals. There are no detectable Pt atoms present on SiO₂-Al₂O₃ to facilitate dehydrogenation or C-C bond cleavage, which differs from Pt/Al₂O₃ materials that likely catalyze tandem hydrogenolysis and aromatization through bifunctional pathways. Here, we hypothesize that acid sites are the active sites for the reaction. To investigate this aspect, a series of SiO₂-Al₂O₃ catalysts of varying silica/alumina ratios (1.5, 5, 10, 20, and 30 wt % SiO₂), comparable surface areas (Table S1), and similar mesopore diameters (Figure S4)—as determined by nitrogen physisorption and small-angle X-ray scattering (SAXS) studies (details are presented in the Supplementary Information, Figures S5-6 and Tables S2-5)—were tested under the previous reaction conditions. The Brønsted and Lewis acid site densities of these catalysts were quantified in a previous work using diffuse-reflectance infrared Fourier transform spectroscopy (DRIFTS) with pyridine adsorption at 180 and 400 °C (Figure S7).³³ Weak (180 °C) and strong (400 °C) Brønsted acid site densities increased with increasing SiO₂ content up to 30% silica due to the formation of acidic Si-O(H)-Al sites, in agreement with previous reports.³⁴ No correlation was observed between silica content and Lewis acid site density.

Upon reacting the series of SiO₂-Al₂O₃ catalysts with polyethylene, clear conversion and product selectivity trends emerged with respect to Brønsted acid site density. The chloroform-

soluble product fraction increased with silica content, while the insoluble fraction decreased (Figure 2a), suggesting chain scission is facilitated by Brønsted acid sites. This is supported by GPC results (Figure 2b)— the chloroform-soluble products progressively decreased in molecular weight with increasing silica/alumina ratio. The aromatic fraction in the products increased with Brønsted acidity as well (defined here as Brønsted acid site density, Figure 2c-d), which aligns with the color changes observed. The products became dark orange due to polyaromatic species as the silica/alumina ratio of the catalyst increased (Figure 2a). Notably, the relative polyaromatic fraction in the ^1H NMR spectrum increased with Brønsted acidity, as evidenced by the growing intensity of the features in the 7.4-9.0 ppm region (Figure 2d) and the decreasing monoaromatic/polyaromatic proton ratio (Figure 2c). We also compared product selectivity for 10SA and 30SA at similar levels of conversion, approximated here by chloroform-soluble product yield and average M_w of the products. Conversion was controlled with reaction time (24 h for 10SA and 6 h for 30SA). Even though both samples had similar total aromatic content at these conversion levels, 10SA produced products with a 3.8 times higher monoaromatic/polyaromatic proton ratio (Table S6).

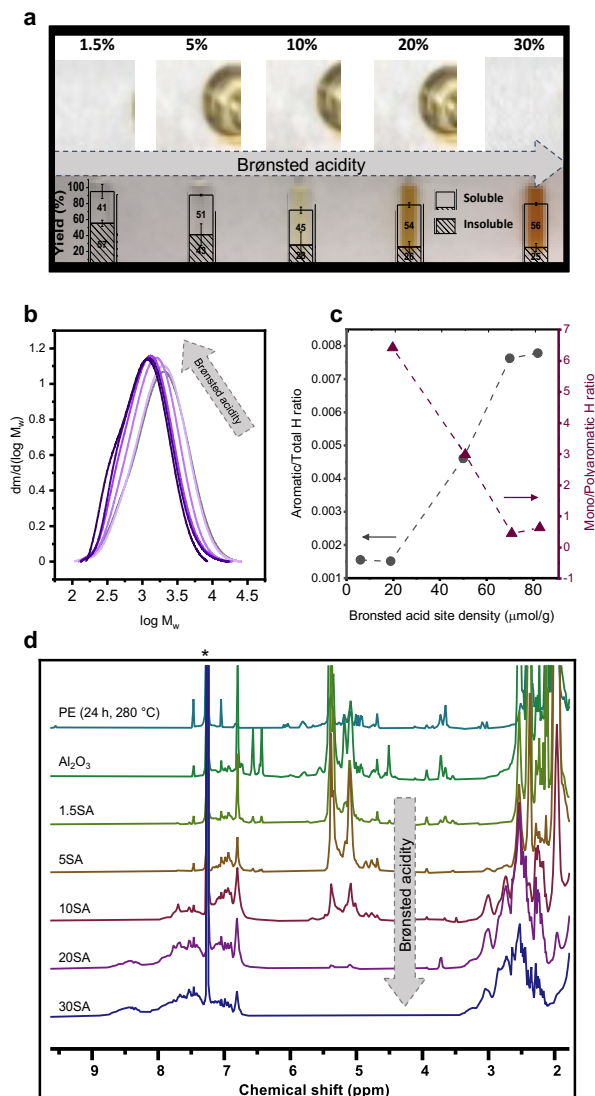


Figure 2. PE deconstruction with SA catalysts of varying silica content (280 °C, 24 h). (a) Reaction vessel interior post-reaction, prior to product extraction (top) and chloroform-extracted products with yield overlay (equivalent concentrations, bottom). Silica content reported as percentage (wt %). (b) GPC profiles, (c) ^1H NMR integrations, and (d) ^1H NMR of chloroform-soluble products reported as a function of Brønsted acid site density. * CDCl_3 solvent signal

Polyethylene chain scission and aromatic formation both appear to be facilitated by Brønsted acid site density under the tested conditions. While the reaction network is likely complex, we hypothesize that these reactions proceed through a carbocation-mediated mechanism akin to acid-catalyzed hydrocarbon cracking, where a series of skeletal rearrangement, hydrogen transfer, and beta-scission steps occur.^{9,35} Analysis of the gaseous reaction products supports this hypothesis. It was found that C3-C5 hydrocarbons were the most abundant species in the gas phase (84%, Figure S8), which is the expected result for monofunctional acid site cracking in which the stability of carbocations determines the formed species.⁹ Hydrogen was also quantified and accounted for 7% of the gaseous products, further suggesting that the reaction created hydrogen via

dehydrogenation reactions on the catalyst. Only trace amounts of methane were detected (1%). This result differs from systems undergoing hydrogenolysis, such as the reaction of PE with Pt/Al₂O₃, where significant amounts of methane are produced.^{9,19} Carbocation-mediated cracking reactions are thought to be initiated over solid acids by either the formation of carbonium species (as described by the Haag-Dessau mechanism for alkane cracking), the formation of carbenium ions via hydride abstraction, or the protonation of olefins in the polyolefin feedstock.^{35–37} While at this time we do not have enough evidence to definitively support a mechanism, we further examined whether the last reason could explain our results.

We see features in the alkene region of the high temperature ¹H NMR spectrum of the PE starting material (commercial, Figure S9), which lends support to the olefin hypothesis. Finding olefins in the polyethylene feedstock was not entirely unexpected. The Phillips ethylene polymerization catalyst, for example, is a common commercial catalyst that creates mono-unsaturated PE chains.³⁸ Hydrogens corresponding to methyne groups are present in our PE feedstock at a concentration of 1700 ppm, as determined from ¹H NMR integration. Assuming an average molecular weight of 3000 g mol⁻¹, this equates to ~1 olefin per every 2.5 molecules of PE. While we cannot rule out contributions from Brønsted and Lewis acid site alkane activation, it is generally accepted that olefins crack faster than paraffins and will follow a traditional cracking mechanism over Brønsted acid sites if present in the feed.^{36,37}

To further investigate the role of pre-existing olefins, reactions were conducted between SiO₂-Al₂O₃ (30 wt % silica, labeled 30SA) and two model compounds: 1-octadecene (ODE) and octadecane. Both are C₁₈ hydrocarbons, but ODE contains a double bond while octadecane does not. Both reactions resulted in C-C bond cleavage, as evidenced by gas chromatography (Figure S10). The reaction that contained pre-existing double bonds, however, yielded products with 6 times higher total aromatic content than the reaction without pre-existing double bonds, and a higher fraction of polyaromatic protons (monoaromatic/polyaromatic proton ratio = 0.8 for ODE and 1.7 for octadecane). These results suggest that the reaction rate is greatly enhanced by the presence of pre-existing olefins in the starting material, as is the case with the PE examined in this study. This is unsurprising given the mechanism for a typical hydrocracking system, where alkenes are first formed on metallic sites before diffusion to acid sites for subsequent cracking reactions.¹² It appears, however, that olefins can form under reaction conditions without a metal catalyst— we observed alkenes in the octadecane reaction products but not in the starting material (Figure S11). Further experiments with PE suggest olefin formation is likely a catalytic process as opposed to thermal; the integrated olefin region of the proton NMR spectrum before and after heating at 280°C for 24 hr without catalyst was almost identical (olefin/paraffin ratio = 0.00178 before heating and 0.00174 after heating).

A pair of experiments were designed to investigate the role of olefins as the reaction proceeds. When the reaction was performed on 30SA using triacontane (*n*-C₃₀H₆₂) as a model compound almost no aromatics were observed by ¹H NMR (Figure S12), and only starting material was observed by GC-MS, suggesting conversion was quite low. By contrast, Zhang *et al.* showed that triacontane with the same purity clearly forms shorter hydrocarbons and aromatics when reacted with Pt/Al₂O₃ under identical conditions, speaking to the fundamental mechanistic

differences between the two systems. When a trace amount of ODE was added to the reactor with triacontane and 30SA, two times greater aromatic content was observed by NMR (Figure S13). GC-MS results, however, suggest that ODE was the predominant species cleaved—peaks appeared at earlier retention times than C18 in the GC spectrum, but no peaks appeared in the region between C18 and C30 (Figure S14). This suggests that metathesis and hydrogen transfer are slow compared to beta-scission cascade reactions under the tested reaction conditions.

We investigated other acidic oxides as potential metal-free catalyst alternatives for polyethylene deconstruction, including titania, HY zeolite, and HZSM-5 zeolite, but none performed as well as $\text{SiO}_2/\text{Al}_2\text{O}_3$. Titania produced mostly chloroform-insoluble products and no aromatics were observed with ^1H NMR (Figure S15), presumably due to a lack of Brønsted acid sites.³⁹ The zeolites, conversely, produced gaseous products almost exclusively, even at short reaction times (3 h). It is possible that the microporous nature of the zeolite inhibits polymer transport, resulting in confinement and over cracking to gaseous products inside the pores.^{12,40} The small fraction of liquid products that could be recovered (17% for HY and 30% for HZSM-5) had up to 10 fold higher aromatic content than reactions with 30SA (Figure S16). This could be attributed to confinement effects or acidity differences, but further studies are required.

Controlling the Brønsted acid site density of the silica alumina is one way to tune the product profile during polyethylene deconstruction, with more acidic catalysts producing a larger fraction of aromatics. We found that the degree of aromatic formation can also be tuned with reaction time and temperature. A non-negligible chloroform-soluble product yield was obtained at temperatures as low as 150 °C after 24 h (Figure 3a) and at reactions times as low as 3 h at 280 °C (Figure 3b) in experiments with 30SA. The insoluble fraction steadily decreased with increasing temperature and reaction time, while the total fraction of aromatics increased. The relative monoaromatic/polyaromatic proton ratio of the products, as determined by ^1H NMR peak integration, was similarly dependent on reaction conditions, decreasing by a factor of 8 over the course of the reaction temperature series. The same trend was observed for the reaction time series, with longer reactions producing a larger fraction of polyaromatic products (Figure S17). The average molecular weight of the chloroform-soluble products also decreased with increasing temperature and reaction time (Figure S18), with the reaction conducted at 150 °C being the one exception. It produced products of a slightly lower molecular weight than was observed at higher temperatures. This may suggest that the reaction proceeds through a different mechanism at 150 °C or that some form of deactivation occurs at elevated temperatures. Further investigations are required. We also tested PE of a higher molecular weight ($M_w \sim 76,000 \text{ g mol}^{-1}$) in a 24 h reaction with 30SA at 280 °C and the ^1H NMR spectrum of the chloroform-soluble products was almost identical to that of low molecular weight PE (Figure S19). Conversion, however, was lower (33% chloroform-soluble yield, 44% chloroform-insoluble yield), as it is expected for running the reaction for the same duration of time.

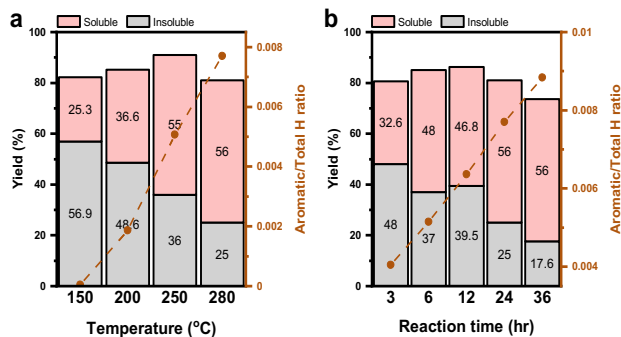


Figure 3. Chloroform-soluble and -insoluble yields with integrations from ^1H NMR. Reactions with 30SA (a) for 24 h at different temperatures and (b) for varying reaction times at 280 °C (all individual experiments)

The Pt/Al₂O₃ system reported by Zhang et al. presumably deactivated after use but could be regenerated via calcination and reduction. We investigated the reusability of 30SA and found instead that chloroform-soluble products were consistently produced over the course of three catalyst recycling events without a reduction in yield (Figure 4). Moreover, the fraction of chloroform-soluble products *increased* as the catalyst was reused. Nanostructural changes were ruled out as a possible explanation, as SAXS measurements of 30SA before and after the reaction did not show appreciable differences in the catalysts (Figure S6 and Table S4). We hypothesize instead that the increase in yield is due to a higher degree of unsaturation in the residual polymer left on the catalyst after the reaction, as compared to the fresh PE, which could conceivably facilitate PE dehydrogenation via transfer hydrogenation. The existence of polymer residues on the used catalyst was confirmed with thermogravimetric analysis and x-ray diffraction (Figures S20-21). The olefins—either in the residual polymer or the fresh PE—are presumably protonated by Brønsted acid sites, forming carbocations that initiate cracking reactions. Thus, a higher degree of unsaturation would lead to more C-C bond cleavage events and an increase in the chloroform-soluble product yield at the expense of chloroform-insoluble products.

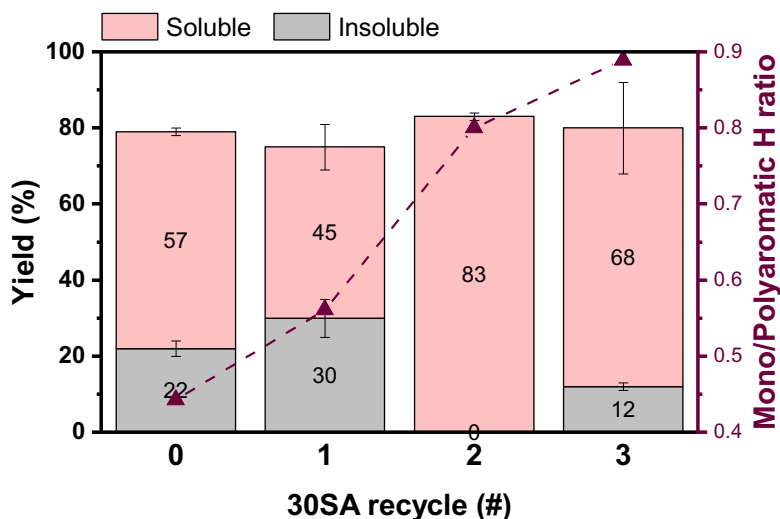


Figure 4. Chloroform-soluble and -insoluble yields with integrations from ^1H NMR for reactions with 30SA (280 °C, 24 h). Catalyst reused 3 times without regeneration

The monoaromatic/polyaromatic proton ratio also increased as the catalyst was reused, doubling over the course of 3 catalyst recycling events. Catalyst deactivation could potentially explain this phenomenon because polyaromatic products are likely formed downstream. We believe the explanation is more nuanced, however, because the total aromatic fraction remained constant over the course of 3 catalyst recycling events (Figure S22), suggesting other changes to the catalyst occur instead of simple deactivation. For example, the increased monoaromatic/polyaromatic proton ratio could be due to a decrease in Brønsted acid strength or density during the reaction, or the deposition of coke on Brønsted acid sites, with aromatic residues that can help withdraw hydrogen atoms from the system. A recent work also postulated that the deposition of polymer residues on Ru/TiO₂ increased the hydrophobicity of the catalyst and led to altered activity upon catalyst reuse.⁴¹ Further studies will be required to differentiate between these possibilities, but the degree of catalyst reuse appears to be another method—in addition to reaction time and temperature—to tune product selectivity.

Conclusion

Clearly, the activity of solid acids for polyolefin deconstruction at low reaction temperatures should not be overlooked. This idea is just starting to gain traction in literature. Lee et al. recently demonstrated, for example, that SiO₂-Al₂O₃, zeolite-Y, and ZSM-5 all have measurable activity for n-hexadecane deconstruction at 275, 325, and 375 °C. Furthermore, the authors found that the activity of the support can dramatically influence the reaction mechanism when metal nanoparticles are dispersed on silica-alumina-based catalysts.⁹ Duan et al. also discovered that ZSM-5 nanosheets catalyze the conversion of polyethylene into light olefins at 280 °C under hydrogen flow conditions.⁴² Herein, we showed that SiO₂-Al₂O₃ is active for

polyethylene deconstruction/aromatization at even lower temperatures, laying the foundation for future studies involving solid acid and bi-functional catalysts. It may be possible, for example, to further facilitate low-temperature polyethylene deconstruction reactions over silica alumina catalysts by introducing unsaturation into the polymer chain, for which there are several established routes.⁴³ This will be examined in future studies.

In this investigation, we demonstrated that SiO₂-Al₂O₃ deconstructs low density polyethylene into shorter, aromatic compounds at sub-pyrolytic temperatures, producing products of similar composition as Pt(1 wt %)/Al₂O₃ without the addition of noble metals or hydrogen. Reactions over SiO₂-Al₂O₃ appear to be facilitated by Brønsted acid sites and product selectivity can be tuned in a variety of ways, including the Brønsted acid site density of the catalyst, reaction time, temperature, and degree of catalyst reuse. There are many advantages to using SiO₂-Al₂O₃ for polyolefin upcycling, including reduced catalyst cost and ease of catalyst reuse. Regeneration steps are not necessary between runs under the investigated conditions, and catalyst activity appears to improve with each use. The recycling landscape is complex but finding inexpensive catalysts for low-temperature conversions to value-added products is a step in the right direction.

Experimental Methods

Materials

Polyethylene ($M_w \sim 3000 \text{ g mol}^{-1}$, SKU-427772; $M_w \sim 76,000 \text{ g mol}^{-1}$, SKU- 428043), triacontane (98%, SKU-263842), octadecane (99%, SKU-O652), 1-octadecene (technical grade, 90%, SKU-O806), chloroform ($\geq 99.8\%$, ReagentPlus®), Pt(1 wt %)/Al₂O₃, and glass microfiber filters (Whatman®, Grade 934-AH®) were obtained from Sigma Aldrich and used as received. Deuterated chloroform (ACROS Organics™, 99.8+ % atom D with 0.03 v/v % TMS), bromobenzene-*d*₅ (Thermo Scientific™, 99% atom D), and Zeolite Y (hydrogen, Alpha Aesar, 780 m²/g, silica:alumina mole ratio = 30:1) were purchased from Fisher Scientific. TiO₂ (Aeroxide, P25) was obtained from Acros and used as received. Al₂O₃ and SiO₂/Al₂O₃ powders of varying SiO₂ content (1.5, 5, 10, 20, and 30 wt %) were obtained from Sasol and used as received.

Polyethylene deconstruction experiments

In a typical reaction, polyethylene (130 mg) and catalyst powders (200 mg) were loaded into stainless steel mini reactors (~10 mL volume) inside an argon glovebox unless stated otherwise. Mini reactors were comprised of 3/4" diameter Swagelok unions and plug fittings following previous reports.^{19,44} The reactors were sealed, removed from the glovebox, and placed in a temperature-controlled furnace pre-heated to reaction temperature (280 °C unless stated otherwise). The temperature fluctuated ± 10 °C upon opening and closing the furnace and remained stable throughout the reaction. Reactors were immediately cooled under a jet of cool air for 15 minutes following the reaction.

The reactor contents were transferred into a pre-weighed glass vial and washed with 20 mL of hot chloroform (50 °C). Chloroform-soluble products were separated from the catalyst powder and chloroform-insoluble residues via vacuum filtration on a glass-fiber filter paper. The catalyst and polymer residue were dried overnight prior to weighing and the chloroform-insoluble yield was calculated as the difference between the recovered mass (catalyst + residual polymer) and initial catalyst mass. Solvent was removed from the chloroform-soluble fraction via rotary evaporation, giving the chloroform-soluble yield.

Characterization

¹H nuclear magnetic resonance (NMR) spectra of chloroform-soluble products and triacontane were collected in chloroform-*d* using a Bruker Neo500 spectrometer (500 MHz) and analyzed using MestReNova software (Version 14.2.0-26256). All product spectra were collected at room temperature and the chemical shifts were referenced to TMS and residual solvent signals. High temperature ¹H NMR of the polyethylene feedstock was collected in bromobenzene-*d*₅ at 80 °C using a Bruker Neo400 spectrometer (400MHz).

High-temperature gel permeation chromatography (HT-GPC) spectra of the starting material and chloroform-soluble products were collected using a Tosoh EcoSEC HT-GPC equipped with a single TSK gel GPC column (GMHHR-H; 300 mm×7.8 mm) and an RI detector. Experiments were run at 180 °C using 1,2,4-trichlorobenzene as the solvent and calibrated against polyethylene standards purchased from Polymer Standards Service encompassing the molecular weight range of the products (840, 1970, and 16,000 Da).

Transmission electron microscopy (TEM) images were recorded on a FEI Tecnai transmission electron microscope equipped with an Orius CCD and a Gatan OneView camera operating at 200 kV. Sample powders were dispersed via dry deposition onto lacey-carbon Cu-mesh TEM grids.

Thermogravimetric analysis (TGA) was performed on a TGA 5500 (TA Instruments). Samples were heated at a rate of 10 °C min⁻¹ under a flow of air (20 mL min⁻¹).

Powder X-ray diffraction (PXRD) spectra were obtained using a Bruker Single Crystal D8 Venture with Mo K α radiation from 5° to 95° 2 θ with a step size of 0.05° and an exposure time of 60 s.

Gas chromatography mass spectrometry (GC-MS) of the liquid products was collected using an Agilent 7890/5975 instrument (single quadrupole MS with an electron impact ionization source) equipped with an HP-5 column ((5 % phenyl)-methylpolysiloxane, 30 m x 0.25 mm x 25 μ m). The following temperature program was used: 35 °C (hold 3.75 min), ramp 20 °C/min to 320 °C (hold 7 min). The flow rate of helium was 1 mL/min, the split ratio was 1:100, and the injector temperature was 280 °C.

Gas chromatography (GC) of the gaseous products was collected with a gas chromatograph (Buck Scientific model 910) using a flame ionization detector (FID) with a methanizer and thermal

conductivity detector (TCD) with Ar as the carrier gas. The following temperature program was used: 60 °C (hold 5 min), ramp 30 °C/min to 150 °C (hold 82 min), ramp 25 °C/min to 250 °C (hold 120 min). Reactions for headspace analysis were conducted in a 50 mL Parr autoclave. The reactor outlet was connected directly to the GC after the reaction was complete and the reactor had cooled to room temperature.

Small-angle X-ray scattering (SAXS) experiments were performed at the 1-5 beamline of The Stanford Synchrotron Radiation Lightsource, SLAC National Laboratory, USA. 1-5 beamline is equipped with a beamstop consisting of an inbuilt diode to measure the transmitted intensity and Pilatus 1M (1024 x 1024 pixels, 172 x 172 μm^2 pixel size; Dectris AG, Switzerland) photon counting area detector. A micro-focused X-ray beam of spot size 300 x 300 μm , 15 keV energy, and sample-to-detector-distance (SDD) of 2.8 m was used in the measurement. SDD was calibrated with the Silver behenate standard powder sample.

Thin wall glass capillaries (1.5 mm diameter, 10 μm wall thickness, manufactured by Hilgenberg GmbH, Germany) were used for powder sample measurement. Each sample and corresponding background (empty capillary) were measured at 3 spots (5 frames of 2 seconds for each spot, total measurement 30 seconds) in transmission mode at room temperature and pressure.

All the frames were averaged in the final analysis of the data. The Igor Pro plugin “Nika” was used for averaging and reducing the data. SAXS data was normalized to the transmitted intensity measured by the beamstop for sample and empty capillary. After normalization, the background (empty capillary and the air) was subtracted from each sample. MATLAB (R2021b) was used for normalization and background subtraction. The Irena packages were used for simulation and analysis of the SAXS profiles.

Supporting information

Catalyst characterization (SAXS, XRD, BET, TGA, TEM), acid site density measurements, NMR and GPC characterization of starting materials/reaction products

Corresponding Author

* mcargnello@stanford.edu

Author Contributions

M.L.P. designed/conducted experiments and wrote the manuscript with conceptual development from M.C. A.K.M, A.M.E, and C.J.T performed the SAXS experiments and analyzed the SAXS and XRD results. All authors edited the manuscript and approved of the final version.

Notes

The authors declare no competing financial interests.

Acknowledgments

M.L.P. gratefully acknowledges support from the National Science Foundation Graduate Research Fellowship under Grant No. DGE-165651. Additional support was provided by the National Science Foundation under grant 1956300. M.C. acknowledges further support from the Sloan Foundation through the Sloan Fellowship. Part of this work was performed at the Stanford Nano Shared Facilities (SNSF), supported by the National Science Foundation under award ECCS-2026822. NMR analysis was funded significantly by the NIH High End Instrumentation grant 1S10OD028697-01. GC-MS analysis was conducted at the Vincent Coates Foundation Mass Spectrometry Laboratory, Stanford University Mass Spectrometry - RRID:SCR_017801. This work was supported in part by NIH P30 CA124435 utilizing the Stanford Cancer Institute Proteomics/Mass Spectrometry Shared Resource. Use of Stanford Synchrotron Radiation Light Source, SLAC National Accelerator Laboratory, is supported by the U.S. Department of Energy, Office of Science, Office of Basic Energy Sciences under Contract No. DE-AC02-76SF00515.

M.L.P. would like to thank Professor David Flaherty for manuscript discussions and the following people for data acquisition support: Stephen Lynch (NMR), Dr. Evan Gardner (XRD), Chengshuang Zhou (TGA), and Pin-Hung Chung (TEM). M.L.P would also like to thank Nicholas Broadbent, Jinwon Oh, and Derek Pennel for project discussions and editing assistance.

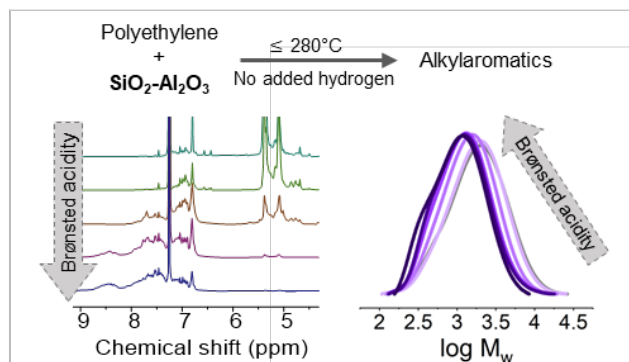
References

- (1) Geyer, R. Production, Use, and Fate of Synthetic Polymers. In *Plastic Waste and Recycling*; Elsevier, 2020; pp 13–32.
- (2) Law, K. L.; Starr, N.; Siegler, T. R.; Jambeck, J. R.; Mallos, N. J.; Leonard, G. H. The United States' Contribution of Plastic Waste to Land and Ocean. *Sci. Adv.* **2020**, *6* (44).
- (3) Environmental Protection Agency. *Advancing Sustainable Materials Management: 2018 Tables and Figures Assessing Trends in Materials Generation and Management in the United States*; 2018.
- (4) Martín, A. J.; Mondelli, C.; Jaydev, S. D.; Pérez-Ramírez, J. Catalytic Processing of Plastic Waste on the Rise. *Chem* **2021**, *7* (6), 1487–1533.
- (5) Jaydev, S. D.; Martín, A. J.; Pérez-Ramírez, J. Direct Conversion of Polypropylene into Liquid Hydrocarbons on Carbon-Supported Platinum Catalysts. *ChemSusChem* **2021**, *14* (23), 5179–5185.
- (6) Rorrer, J. E.; Beckham, G. T.; Román-Leshkov, Y. Conversion of Polyolefin Waste to Liquid Alkanes with Ru-Based Catalysts under Mild Conditions. *JACS Au* **2021**, *1* (1), 8–12.
- (7) Celik, G.; Kennedy, R. M.; Hackler, R. A.; Ferrandon, M.; Tennakoon, A.; Patnaik, S.; LaPointe, A. M.; Ammal, S. C.; Heyden, A.; Perras, F. A.; Pruski, M.; Scott, S. L.; Poepelmeier, K. R.; Sadow, A. D.; Delferro, M. Upcycling Single-Use Polyethylene into High-Quality Liquid Products. *ACS Cent. Sci.* **2019**, *5* (11), 1795–1803.
- (8) Chen, S.; Tennakoon, A.; You, K. E.; Paterson, A. L.; Yappert, R.; Alayoglu, S.; Fang, L.; Wu, X.; Zhao, T. Y.; Lapak, M. P.; Saravanan, M.; Hackler, R. A.; Wang, Y. Y.; Qi, L.; Delferro, M.; Li, T.; Lee, B.; Peters, B.; Poepelmeier, K. R.; Ammal, S. C.; Bowers, C. R.; Perras, F. A.; Heyden, A.; Sadow, A. D.; Huang, W. Ultrasmall Amorphous Zirconia Nanoparticles Catalyze Polyolefin Hydrogenolysis. *Nat. Catal.* **2023**, *6* (2), 161–173.
- (9) Lee, W.-T.; van Muyden, A.; Bobbink, F. D.; Mensi, M. D.; Carullo, J. R.; Dyson, P. J. Mechanistic Classification and Benchmarking of Polyolefin Depolymerization over Silica-Alumina-Based Catalysts. *Nat. Commun.* **2022**, *13* (1), 4850.
- (10) Tennakoon, A.; Wu, X.; Paterson, A. L.; Patnaik, S.; Pei, Y.; LaPointe, A. M.; Ammal, S. C.; Hackler, R. A.; Heyden, A.; Slowing, I. I.; Coates, G. W.; Delferro, M.; Peters, B.; Huang, W.; Sadow, A. D.; Perras, F. A. Catalytic Upcycling of High-Density Polyethylene via a Processive Mechanism. *Nat. Catal.* **2020**, *3* (11), 893–901.
- (11) Liu, S.; Kots, P. A.; Vance, B. C.; Danielson, A.; Vlachos, D. G. Plastic Waste to Fuels by Hydrocracking at Mild Conditions. *Sci. Adv.* **2021**, *7* (17), 8283–8304.
- (12) Kots, P. A.; Vance, B. C.; Vlachos, D. G. Polyolefin Plastic Waste Hydroconversion to Fuels, Lubricants, and Waxes: A Comparative Study. *React. Chem. Eng.* **2022**, *7* (1), 41–54.
- (13) Chen, L.; Zhu, Y.; Meyer, L. C.; Hale, L. V.; Le, T. T.; Karkamkar, A.; Lercher, J. A.; Gutiérrez, O. Y.; Szanyi, J. Effect of Reaction Conditions on the Hydrogenolysis of Polypropylene and Polyethylene into Gas and Liquid Alkanes. *React. Chem. Eng.* **2022**, *7* (4), 844–854.
- (14) Hackler, R. A.; Lamb, J. V.; Peczak, I. L.; Kennedy, R. M.; Kanbur, U.; LaPointe, A. M.; Poepelmeier, K. R.; Sadow, A. D.; Delferro, M. Effect of Macro- and Microstructures on Catalytic Hydrogenolysis of Polyolefins. *Macromolecules* **2022**, *55* (15), 6801–6810.
- (15) Tamura, M.; Miyaoka, S.; Nakaji, Y.; Tanji, M.; Kumagai, S.; Nakagawa, Y.; Yoshioka, T.; Tomishige, K. Structure-Activity Relationship in Hydrogenolysis of Polyolefins over Ru/Support Catalysts. *Appl. Catal. B Environ.* **2022**, *318*, 121870.
- (16) Wang, C.; Xie, T.; Kots, P. A.; Vance, B. C.; Yu, K.; Kumar, P.; Fu, J.; Liu, S.; Tsilomelekis, G.; Stach, E.

- A.; Zheng, W.; Vlachos, D. G. Polyethylene Hydrogenolysis at Mild Conditions over Ruthenium on Tungstated Zirconia. *JACS Au* **2021**, *1* (9), 1422–1434.
- (17) Rorrer, J. E.; Troyano-Valls, C.; Beckham, G. T.; Román-Leshkov, Y. Hydrogenolysis of Polypropylene and Mixed Polyolefin Plastic Waste over Ru/C to Produce Liquid Alkanes. *ACS Sustain. Chem. Eng.* **2021**, *9* (35), 11661–11666.
- (18) Anuar Sharuddin, S. D.; Abnisa, F.; Wan Daud, W. M. A.; Aroua, M. K. A Review on Pyrolysis of Plastic Wastes. *Energy Convers. Manag.* **2016**, *115*, 308–326.
- (19) Zhang, F.; Zeng, M.; Yappert, R. D.; Sun, J.; Lee, Y.-H.; LaPointe, A. M.; Peters, B.; Abu-Omar, M. M.; Scott, S. L. Polyethylene Upcycling to Long-Chain Alkylaromatics by Tandem Hydrogenolysis/Aromatization. *Science*. **2020**, *370* (6515), 437–441.
- (20) Vollmer, I.; Jenks, M. J. F.; Roelands, M. C. P.; White, R. J.; Harmelen, T. van; Wild, P. de; Laan, G. P. van der; Meirer, F.; Keurentjes, J. T. F.; Weckhuysen, B. M. Beyond Mechanical Recycling: Giving New Life to Plastic Waste. *Angew. Chemie Int. Ed.* **2020**, *59* (36), 15402–15423.
- (21) Chen, Z.; Xu, L.; Zhang, X. Upgrading of Polyethylene to Hydrocarbon Fuels over the Fe-Modified Pt/Al₂O₃ Catalysts at a Mild Condition without External H₂. *Chem. Eng. J.* **2022**, *446*, 136213.
- (22) Lopez, G.; Artetxe, M.; Amutio, M.; Bilbao, J.; Olazar, M. Thermochemical Routes for the Valorization of Waste Polyolefinic Plastics to Produce Fuels and Chemicals. A Review. *Renew. Sustain. Energy Rev.* **2017**, *73*, 346–368.
- (23) Pyra, K.; Tarach, K. A.; Góra-Marek, K. Towards a Greater Olefin Share in Polypropylene Cracking – Amorphous Mesoporous Aluminosilicate Competes with Zeolites. *Appl. Catal. B Environ.* **2021**, *297*.
- (24) Ochoa, R.; Van Woert, H.; Lee, W. H.; Subramanian, R.; Kugler, E.; Eklund, P. C. Catalytic Degradation of Medium Density Polyethylene over Silica-Alumina Supports. *Fuel Process. Technol.* **1996**, *49*, 119–136.
- (25) Liu, S.; Kots, P. A.; Vance, B. C.; Danielson, A.; Vlachos, D. G. Plastic Waste to Fuels by Hydrocracking at Mild Conditions. *Sci. Adv.* **2021**, *7* (17), 8283–8304.
- (26) Aguado, J.; Sotelo, J. L.; Serrano, D. P.; Calles, J. A.; Escola, J. M. Catalytic Conversion of Polyolefins into Liquid Fuels over MCM-41: Comparison with ZSM-5 and Amorphous SiO₂ - Al₂O₃. *Energy and Fuels* **1997**, *11* (6), 1225–1230.
- (27) Meriaudeau, P.; Naccache, C. Dehydrocyclization of Alkanes Over Zeolite-Supported Metal Catalysts: Monofunctional or Bifunctional Route. *Catal. Rev.* **1997**, *39*, 5–48.
- (28) Aguado, J.; Serrano, D. P.; Romero, M. D.; Escola, J. M. Catalytic Conversion of Polyethylene into Fuels over Mesoporous MCM-41. *Chem. Commun.* **1996**, No. 6, 725–726.
- (29) Ohkita, H.; Nishiyama, R.; Tochihara, Y.; Mizushima, T.; Kakuta, N.; Morioka, Y.; Ueno, A.; Namiki, Y.; Tanifuji, S. Acid Properties of Silica-Alumina Catalysts and Catalytic Degradation of Polyethylene. *Ind. Eng. Chem. Res.* **1993**, *32* (12), 3112–3116.
- (30) Bin Jumah, A.; Malekshahian, M.; Tedstone, A. A.; Garforth, A. A. Kinetic Modeling of Hydrocracking of Low-Density Polyethylene in a Batch Reactor. *ACS Sustain. Chem. Eng.* **2021**, *9* (49), 16757–16769.
- (31) Mark, L. O.; Cendejas, M. C.; Hermans, I. The Use of Heterogeneous Catalysis in the Chemical Valorization of Plastic Waste. *ChemSusChem* **2020**, *13* (22), 5808–5836.
- (32) He, Y.; Qiu, X.; Klosin, J.; Cong, R.; Roof, G. R.; Redwine, D. Terminal and Internal Unsaturation in Poly(Ethylene-Co-1-Octene). *Macromolecules* **2014**, *47* (12), 3782–3790.
- (33) Yang, A. C.; Zhu, H.; Li, Y.; Cargnello, M. Support Acidity Improves Pt Activity in Propane Combustion in the Presence of Steam by Reducing Water Coverage on the Active Sites. *ACS Catal.* **2021**, *11*, 6672–6683.
- (34) Mouat, A. R.; George, C.; Kobayashi, T.; Pruski, M.; Van Duyne, R. P.; Marks, T. J.; Stair, P. C. Highly

- Dispersed SiO_x/Al₂O₃ Catalysts Illuminate the Reactivity of Isolated Silanol Sites. *Angew. Chemie Int. Ed.* **2015**, *54* (45), 13346–13351.
- (35) Weitkamp, J. Catalytic Hydrocracking—Mechanisms and Versatility of the Process. *ChemCatChem* **2012**, *4* (3), 292–306.
- (36) Kotrel, S.; Knözinger, H.; Gates, B. C. The Haag–Dessau Mechanism of Protolytic Cracking of Alkanes. *Microporous Mesoporous Mater.* **2000**, *35–36*, 11–20.
- (37) Wojciechowski, B. W.; Corma, A. *Catalytic Cracking: Catalysts, Chemistry, and Kinetics*; Marcel Dekker Inc., New York, NY, 1986.
- (38) Wang, N. M.; Strong, G.; DaSilva, V.; Gao, L.; Huacuja, R.; Konstantinov, I. A.; Rosen, M. S.; Nett, A. J.; Ewart, S.; Geyer, R.; Scott, S. L.; Guironnet, D. Chemical Recycling of Polyethylene by Tandem Catalytic Conversion to Propylene. *J. Am. Chem. Soc.* **2022**, *144* (40), 18526–18531.
- (39) Doolin, P. K.; Alerasool, S.; Zalewski, D. J.; Hoffman, J. F. Acidity Studies of Titania-Silica Mixed Oxides. *Catal. Letters* **1994**, *25* (3–4), 209–223.
- (40) Zhang, Z.; Gora-Marek, K.; Watson, J. S.; Tian, J.; Ryder, M. R.; Tarach, K. A.; López-Pérez, L.; Martínez-Triguero, J.; Melián-Cabrera, I. Recovering Waste Plastics Using Shape-Selective Nano-Scale Reactors as Catalysts. *Nat. Sustain.* **2019**, *2* (1), 39–42.
- (41) Wang, K.; Jia, R.; Cheng, P.; Shi, L.; Wang, X.; Huang, L. Highly Selective Catalytic Oxi-upcycling of Polyethylene to Aliphatic Dicarboxylic Acid under a Mild Hydrogen-Free Process. *Angew. Chemie* **2023**, *135* (29), e202301340.
- (42) Duan, J.; Chen, W.; Wang, C.; Wang, L.; Liu, Z.; Yi, X.; Fang, W.; Wang, H.; Wei, H.; Xu, S.; Yang, Y.; Yang, Q.; Bao, Z.; Zhang, Z.; Ren, Q.; Zhou, H.; Qin, X.; Zheng, A.; Xiao, F.-S. Coking-Resistant Polyethylene Upcycling Modulated by Zeolite Micropore Diffusion. *J. Am. Chem. Soc.* **2022**, *144* (31), 14269–14277.
- (43) Arroyave, A.; Cui, S.; Lopez, J. C.; Kocen, A. L.; Lapointe, A. M.; Delferro, M.; Coates, G. W. Catalytic Chemical Recycling of Post-Consumer Polyethylene. *J. Am. Chem. Soc.* **2022**, *144* (51), 23280–23285.
- (44) Macala, G. S.; Matson, T. D.; Johnson, C. L.; Lewis, R. S.; Iretskii, A. V.; Ford, P. C.; Macala, S.; Matson, T. D.; Lewis, R. S.; Ford, P. C.; Johnson, C. L.; Iretskii, A. V. Hydrogen Transfer from Supercritical Methanol over a Solid Base Catalyst: A Model for Lignin Depolymerization. *ChemSusChem* **2009**, *2* (3), 215–217.

For table of contents (TOC):



Synopsis:

Mesoporous silica-alumina converts polyethylene plastic into tunable aromatic compounds at sub-pyrolytic temperatures without the use of metals or added hydrogen.